Uncertainty-informed selection of CMIP6 Earth System Model subsets for use in multisectoral and impact models

Abigail Snyder[1], Noah Prime[1,] Claudia Tebaldi[1], Kalyn Dorheim[1]

[1]Pacific Northwest National Laboratory, Joint Global Change Research Institute, College Park MD, 20740, USA

Correspondence to: Abigail Snyder (abigail.snyder@pnnl.gov)

Abstract. Earth System Models (ESMs) and General Circulation Models (GCMs) are heavily used to provide inputs to sectoral impact and multisectoral dynamic models, which include representations of energy, water, land, economics, and their interactions. Therefore, representing the full range of model uncertainty, scenario uncertainty, and interannual variability that ensembles of these models capture is critical to the exploration of the future co-evolution of the integrated human-Earth system. The pre-eminent source of these ensembles has been the Coupled Model Intercomparison Project (CMIP). With more modeling centers participating in each new CMIP phase, the size of the model archive is rapidly increasing, which can be intractable for impact modelers to effectively utilize due to computational constraints and the challenges of analyzing large datasets. In this work, we present a method to select a subset of the latest phase, CMIP6, models for use as inputs to a sectoral impact or multisectoral models, while prioritizing preservation of the range of model uncertainty, scenario uncertainty, and interannual variability of the full CMIP6 ESM results. This method is intended to help human-relevant impact and multisectoral modelers select climate information from the CMIP archive efficiently for use in downstream models that require global coverage of climate information. This is particularly critical for large ensemble experiments of multisectoral dynamic models that may be varying additional features beyond climate inputs in a factorial design, thus putting constraints on the number of climate simulations that can be used. We focus on temperature and precipitation outputs of CMIP6 models as these are two of the most used variables among impact models and many other key input variables for impacts are at least correlated with one or both of temperature and precipitation (e.g. relative humidity). Besides preserving the multi-model ensemble variance characteristics, we prioritize selecting CMIP6 models in the subset that preserve the very likely distribution of equilibrium climate sensitivity values as assessed by the latest IPCC report. This approach could be applied to other output variables of climate models and, when combined with emulators, offers a flexible framework for designing more efficient experiments on human-relevant climate impacts. It can also provide greater insight into the properties of existing CMIP6 models.

1 Introduction

The future evolution of the integrated human-Earth system is highly uncertain, but one common approach to begin addressing this uncertainty is to use outputs from a variety of computationally expensive, highly detailed process-based Earth System Models (ESMs) and General Circulation Models (GCMs) run under different scenarios. This approach has been facilitated by the Coupled Model Intercomparison Project (CMIP) (Eyring et al. 2016), which has organized experiments that are standardized across modeling centers. Scenario simulations from CMIP (most recently through ScenarioMIP, (O'Neill et al. 2016) are commonly used as inputs to downstream sectoral impact and multisector dynamic models, both by individual modeling efforts and by large, coordinated impact

Deleted:

Deleted: ESMs

Deleted: ,

Deleted: ESM

Deleted: still representing

Deleted: ESMs,

Deleted: ESMs

Deleted: ESMs

Deleted: ESMs and the method may be informative for future experiment planning across ESMs.

Deleted:

modeling projects, like AgMIP or ISIMIP (e.g. (Rosenzweig et al. 2013; Rosenzweig et al. 2014; Warszawski et al. 2014; Frieler et al. 2017)). Using such multi-model ensembles captures the process and structural uncertainties represented by sampling across ESM/GCMs, scenario uncertainty, and, to the extent that an ESM/GCM runs multiple initial condition ensemble members for a scenario, internal variability of the individual ESM (Hawkins and Sutton 2009; Hawkins and Sutton 2011; Lehner et al. 2020). These Earth system uncertainties can then be propagated through an impact model (perhaps after bias-correction (Lange 2019)) to understand possible human-relevant outcomes.

From the Earth system modelers who produce climate data to the impact and multisectoral dynamic modelers who use it, each step in this process is computationally expensive. For Earth system modelers, variability across ESM/GCMs' projections of future climate variables can be significant (Hawkins and Sutton 2009; Hawkins and Sutton 2011; Lehner et al. 2020) and so the participation of multiple modeling centers running multiple scenarios is critical to understanding the future of the Earth system. Further, statistical evaluation (Tebaldi et al. 2021) suggests that 20-25 initial condition ensemble members for each scenario an ESM/GCM provides are needed to estimate the forced component of extreme metrics related to daily temperature and precipitation, which are key inputs to many impacts models covering hydrological, agricultural, energy and other sectors. Fortunately, emulation of ESM/GCM outputs to infill missing scenarios and enrich initial condition ensembles continues to improve (Beusch, Gudmundsson, and Seneviratne 2020; Nath et al. 2022; Quilcaille et al. 2022; Tebaldi, Snyder, and Dorheim 2022). This suggests that ESM/GCMs don't necessarily have to provide all of the runs desired for capturing possible futures, but instead a subset of scenarios including initial condition ensembles for emulator training. The total burden across the modeling and analysis community to sample across ESM/GCMs and scenarios still remains high, even with the potential efficiency provided by emulators. Downstream from the physical climate science community, impact modelers often seek to understand future climate impacts in the context of ESM uncertainty by using the outputs of multiple ESMs under multiple scenarios as inputs to impact models (e.g. (Prudhomme et al. 2014; Müller et al. 2021)). In a world unburdened by time and computing constraints, an impact model would take as input every projected data set available (possibly weighted according to observation and/or by model independence) to have a full understanding of the total variance in possible outcomes. Our world includes those burdens, made even larger when impact models require bias-corrected climate data as input. This can quickly become an intractably-sized set of runs to perform and analyze for impact modelers. For the multisectoral dynamics community, whose modelers often attempt to integrate results from multiple impact models to understand interactions of different sectors (like energy, water, land, and economics) of the integrated human-Earth system (Graham et al. 2020) this challenge multiplies. Finally, multisectoral dynamic models are beginning to run large ensemble experiments that vary additional features beyond climate inputs in a factorial design (e.g. (Dolan et al. 2021, 2022; Guivarch et al. 2022)) further adding to the computational costs to be faced. The multisectoral dynamics approach is the approach that the examples in this work focus on: downstream models that require global coverage of a variety of climate model output variables at different temporal scales. Were a study to be focused on particular regions or localized impacts and dynamics, other selection criteria, such as model skill (closeness to observation, ability to replicate modes of variability known to be particularly important to that region, etc.) and the effect of downscaling and bias

Deleted:

Deleted: However the

Deleted: centers

Deleted: is

Deleted: I

Deleted:

Deleted: and

Deleted: input

Deleted: , the computational expense for impact modelers and the broader community only grows. …

correction, known to introduce additional sources of variability and uncertainty (Lafferty and Sriver 2023) in that region could be explored.

For all communities involved, an efficient way to design and then use climate model runs is critical. While there is likely no perfect solution to balance the tension between the competing priorities of different climate data creators and climate data users, this work describes a method for selecting a subset of CMIP6 models that prioritizes faithfully representing the uncertainty characteristics of the entire data set, particularly in dimensions relevant to impact and multisectoral modelers. The method proposed here exists in the context of a rich literature on model selection, with methods focused on model skill in comparison to observation and/or tracking and controlling for climate model dependence (Abramowitz et al. 2019; Brands 2022; Merrifield et al. 2023; Parding et al. 2020). These are critical aspects to consider when sub-selecting climate models for downstream use. Merrifield et al (2023) does include model spread as a critical consideration for model selection, but to our knowledge, there is no uncertainty-first consideration of climate model selection. The method we present in this work is an adaptable framework that could complement other approaches based on skill and climate model independence, and some of the choices made in implementing this method may be adaptable for other uses or priorities.

2 Methods

We approach the question of uncertainty in the full collection of CMIP6 models as being one of understanding the total variance in the CMIP6 outputs, following the Hawkins and Sutton framing of the problem (Hawkins and Sutton 2009; Hawkins and Sutton 2011; Lehner et al. 2020). Rather than attributing fractions of total variance to different sources and optimizing that as part of the selection process, however, we focus on projecting the data into a new coordinate basis designed to maximize total variance. Principal Component Analysis (PCA) does exactly this: it identifies a new set of basis vectors maximizing total variance that data can be projected into. Once climate model data has been projected into this space (e.g. as in Figure 3), it's straightforward to sample climate models that span the projections of the full set of climate model outputs.

The overall steps of this method are summarized in Table 1. Sections 2.1 and 2.2 provide fuller details on using PCA to characterize the full set of climate model data (2.1) and selecting a representative subset of climate models within that characterization (2.2). Table 1 especially highlights the choices made for this particular effort, based on the authors' experience with multisectoral impact modeling. Section 2.3 outlines our approach to evaluating the extent to which our model subset preserves the uncertainty properties of the full data set. Nothing in method prevents its being adapted with different regions of interest, indices of behavior, or ESM/GCM output variables, although evaluation of results in new implementations would be necessary.

Table 1. Summary of method

Deleted: ESM

Deleted: se

Deleted: s

Deleted: till

Deleted: s

Deleted: The subset of ESMs outlined here is merely one approach to make understanding the future of the human-Earth system more tractable. The calculations described in this paper may also serve as a useful characterization of ESM behavior for modelers in other contexts. Finally, many of the choices made in implementing this method may be adaptable for other uses or priorities. We also briefly discuss ways that this work can be leveraged by Earth system modelers in future comparison exercises to more efficiently identify specific ESMs to focus on larger initial condition ensembles.

Formatted: Normal

Deleted: 2

Deleted: building up the method and justifying choices

Deleted: 2

Deleted: It is likely that the approach could be adapted

Deleted: validation

Deleted: these cases

Step	Description	Experiment 1	Experiment 2
1	Identify relevant climate model output variables	Temperature, precipitation from all (22) ScenarioMIP Tier 1-participating models	Temperature, precipitation from independent* (16) ScenarioMIP Tier 1-participating models
2	Aggregate gridded time series to region-levels	IPCC WG1 non-arctic land	IPCC WG1 non-arctic land
3	Identify and extract region indices for each variable, for each Model-Scenario to capture characteristics of uncertainty of interest	Ensemble averaged: mid-century anomaly, end of century anomaly, interannual standard deviation	Ensemble averaged: mid-century anomaly, end of century anomaly, interannual standard deviation
4	Form a matrix of Model*Scenario rows and Region*Indices columns for the full data and perform PCA; identify number of eigenvectors, *N*, responsible for majority of variance	*N=5* eigenvectors	*N=5* eigenvectors
5	Create candidate subsets of models based on heuristic filters of interest	Model subset size = 5; heuristic filter is that each subset must preserve the IPCC distribution of equilibrium climate sensitivity.	Model subset size = 5; heuristic filter is that each subset must preserve the IPCC distribution of equilibrium climate sensitivity.
6	Calculate the summary metric for each subset and select the subset with the smallest value	Minimize distance from out-of-subset model to a subset model across the *N=5* dimensions.	Minimize distance from out-of-subset model to a subset model across the *N=5* dimensions.
7	Calculate the Hawkins and Sutton partitions for the full set of data and selected subset and use as independent, qualitative evaluation data	Full data = 22 models Subset = ACCESS-CM2, ACCESS-ESM1-5, CMCC-ESM2, MRI-ESM2-0, GFDL-ESM4	Full data = 16 models Subset = IPSL-CM6A-LR, ACCESS-ESM1-5, MRI-ESM2-0, BCC-CSM2-MR, MIROC6
	* independent as defined in this work, many definitions exist		

2.1 Data preparation and characterization

Impact models often require multiple output variables from a climate model on daily or monthly time scales, with temperature and precipitation being the most common variables needed. For tractability, we focus on the IPCC WG1 non-arctic land regions (Iturbide et al. 2022), as these regions are primarily where humans live, consume water, generate electricity, and grow food. I.e., the places most relevant in multisectoral models of the integrated human-Earth system. We also limit ourselves to ESM/GCMs that completed all four ScenarioMIP Tier 1 experiments (Table 2). This still results in more than 600 trajectories across models, scenarios, and ensemble members for each region.

In this work, we are treating this collection of ESM/GCMs and scenario results in these regions as the full set of data of which we would like to faithfully represent the uncertainty characteristics, and then select a subset of climate models for impact modelers to use, based on preserving those characteristics. Critically, however, is that once the full set of climate data is characterized, as we outline in this section, the selection step of the method includes a step to restrict the ECS distribution of the model subset to reflect that of the IPCC AR6-defined most likely distribution (Core Writing Team, H. Lee and J. Romero (eds.) 2023). This shifts the average ECS value of the selected subset down relative to the existing full data covered in Table 2Table 3Table 1. Following this ECS distribution, a single high ECS climate model is allowed to be included in the subset, allowing both the 'hot model problem' (Hausfather et al. 2022) to be addressed as part of the model subset selection process as well as ensuring that a range of model behaviors across different ECS values are included. Models for which we could not readily identify ECS values in the literature are included in the characterization of the full space but they are not eligible for selection in the subset, as preserving the IPCC distribution of ECS values is a critical filter in this selection process for the examples outlined in this work (more details in Section 2.2).

Table 2. Models and scenarios making up the full set of data, as well as their equilibrium climate sensitivity (ECS) values sourced from *(Meehl et al. 2020; Lovato et al. 2022)*. Note that even the Earth System Models in CMIP6 run these experiments in concentration-driven mode rather than emissions-driven mode.

ESM	ECS	SSP126 Ensemble size	SSP245 Ensemble size	SSP370 Ensemble size	SSP585 Ensemble size
ACCESS-CM2	4.7	5	5	5	5
ACCESS-ESM1-5	3.9	40	10	30	40
BCC-CSM2-	3.0	1	1	1	1

Deleted: n ESM

Deleted: 1

Deleted: ESMs

Formatted: Default Paragraph Font, Font color: Black

Deleted: ¶

Deleted: 1

Deleted: *; Scafetta 2022*

MR					
CAMS-CSM1-0	2.3	2	2	2	2
CESM2	5.2	3	3	3	3
CESM2-WACCM	4.8	1	3	1	3
CMCC-CM2-SR5	NA	1	1	1	1
CMCC-ESM2	3.57	1	1	1	1
CanESM5	5.6	25	25	25	25
EC-Earth3-Veg-LR	NA	3	3	3	3
FGOALS-f3-L	3.0	1	1	1	1
FGOALS-g3	NA	4	4	4	4
GFDL-ESM4	2.6	1	3	1	1
INM-CM4-8	1.8	1	1	1	1
INM-CM5-0	1.9	1	1	5	1
IPSL-CM6A-LR	4.6	6	11	11	6
MIROC6	2.6	50	33	3	50
MPI-ESM1-2-HR	3.0	2	2	10	2
MPI-ESM1-2-LR	3.0	10	10	10	10
MRI-ESM2-0	3.2	5	5	5	5
NorESM2-MM	NA	1	2	1	1
UKESM1-0-LL	5.3	13	14	13	5

Deleted: 3.52

Deleted: 2.5

For each scenario, region, and available ensemble member in each in each ESM/GCM, we extract the following ensemble-average temperature and precipitation outputs: mid-century (2040-2059) average anomaly relative to that model's historical average (1995-2014), the end of century (2080-2099) anomaly relative to historical average, and the interannual standard deviation. Interannual standard deviation is calculated by detrending the regional average level temperature and precipitation time series from 1994-2100 using non-parametric locally weighted smoothing (LOESS as implemented in the python statsmodels package), and then taking the standard deviation of the residuals. For each scenario and model, these ensemble-member values are used to calculate the ensemble average to form our final indices in each region. These six indices (three for each of temperature and precipitation) per ESM-scenario-region combination are selected to result in data that represents the model uncertainty, scenario uncertainty, and interannual variability of our full set of data. By focusing on ensemble averages, models that performed more realizations are not over-represented in the overall space. When an ensemble size is only one realization, that realization's value is used. The key question is how to efficiently characterize this collection of data in a way that enables an efficient subsampling of models that still preserves the main dimensions of variations of the full ensemble.

This full data can be written as a matrix $\boldsymbol{A}$ with *Nmodel*Nscenarios* rows and *Nindices*Nregions* columns. In the case of considering all 22 models listed in Table 2 as representative of the full space, this is 88 rows and 258 columns and we use these numbers for simplicity in some of the vector descriptions that follow. Below, we outline two experiments that highlight the adaptability of this method by considering model dependency in the CMIP6 models versus not. In the case of restricting to independent models only to make up the full data, these numbers of course change.

Principal components analysis (PCA) is then a natural technique to understand the variance of this full data set by forming the covariance matrix $\boldsymbol{S} = \boldsymbol{A}^T\boldsymbol{A}$. The eigenvectors of $\boldsymbol{S}$ are a set of orthogonal basis vectors (each vector is length 258) that are ordered by how much variance of the full data each eigenvector explains. Mathematically, this means that each row of $\boldsymbol{A}$, $(\{\vec{a_i} | i = 1 \dots 88\})$ representing the indices in all regions for a single climate model-scenario) can be projected into the space of eigenvectors $\{\vec{PC_i} | i = 1 \dots 88\}$ and written as $\vec{a_i} = \Sigma_j c_{ij} \vec{PC_j}$ for projection coefficients (coordinates in the basis of eigenvectors), c_{ij}. Thus $\vec{PC_1}$, for example represents some pattern of joint, spatiotemporal temperature and precipitation behaviors that explains the greatest variance across ESM/GCM-scenario observations. Each CMIP6 model-scenario combination has some contribution from this pattern described by its projection coefficient, c_{i1}. This projection can be done over all eigenvectors, or as is common with PCA, a small subset of the eigenvectors that explain the majority of variance.

To demonstrate the flexibility of this approach to characterizing data, we perform the same analysis in two different experiments:

- Experiment 1 assumes all 22 models listed in Table 2 make up the full data.

Deleted: and

Deleted:

Deleted: ESM

Deleted: then,

Deleted: suggests

Deleted: *22 ESM * 4 Scenarios =88* rows and *6 indices * 43 IPCC regions = 258* columns.…

Formatted: Normal (Web)

Deleted: ESM

- Experiment 2 assumes the full data is made up of only 16 of the models in Table 2Table 3Table 1, with ACCESS-CM2, CESM2-WACCM, CMCC-CM2-SR5, FGOALS-f3-L, INM-CM4-8, and MPI-ESM1-2-HR being removed from consideration as they share clear model dependencies with other models in the full data. When deciding which of two related models to keep, we chose based on keeping the model with greater number of realizations as this is valuable for downstream uses. Other criteria could be used to define model dependency and make selections, as determining model independence is itself a rich field of study (Abramowitz et al. 2019; Brands 2022; Merrifield et al. 2023).

Figure 1 is a plot of the fraction of variance explained by each of the first 15 eigenvectors in each experiment. Based on this figure, we restrict ourselves to the first five eigenvectors for projections (just after the 'elbow'), explaining more than 70% of total variance for each experiment. The number of eigenvectors considered is another area of flexibility of this method.

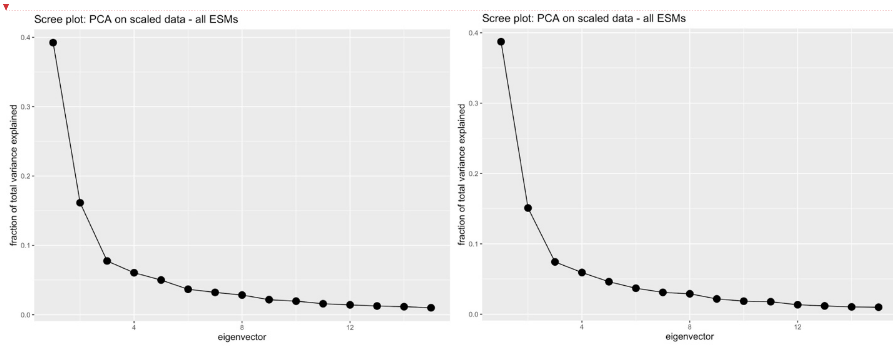

Figure 1: fraction of variance explained by each eigenvector for Experiment 1 (left) and Experiment 2 (right) **for the first 15 eigenvectors.**

Figure 2 is a visual representation of these five eigenvectors for each experiment. Each row is a map of all indices for each eigenvector. For both experiments $\overrightarrow{PC_1}$ is dominated by temperature and, to a lesser extent, high latitude precipitation, highlighting that these features are responsible for 38.7% of the total variance of our full set of data (from Fig. 1). $\overrightarrow{PC_2}$ is dominated by temperature interannual variability and high latitude precipitation interannual variability. $\overrightarrow{PC_3}$ to $\overrightarrow{PC_5}$ feature a mix of the indices, with strong emphasis on precipitation related behaviors. Note that because we treated temperature and precipitation indices together in one matrix, the eigenvectors include joint temperature-precipitation behaviors that may be missed if the variables were treated separately. When comparing each map between the two experiments, it is worth noting that the spatial patterns are strikingly similar. This suggests that the patterns of total variance in this data set are dominated by differences beyond those that might be captured in our definition of model dependence. For example, maybe different

Deleted: , explaining 71.8% of variance. ¶

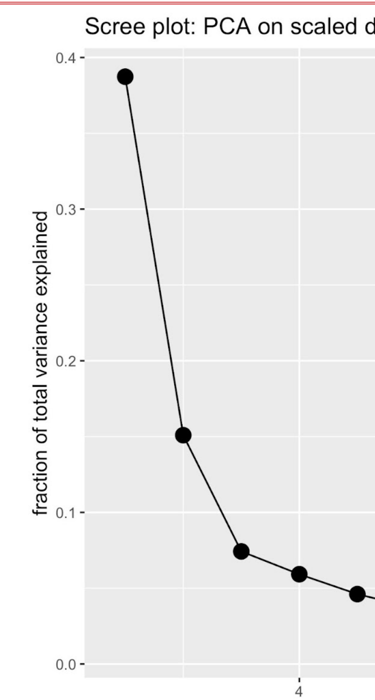

Deleted:

Deleted: the full set of data

Deleted: six

representations of ocean physics are playing a large role. Testing of this hypothesis is outside the scope of this method description work but highlights the potential value of characterizing an archive of CMIP data in this way. In Figures 1 and 3, we also see that the fraction of total variance explained by each eigenvector is similar across the two experiments. Overall, this similarity when accounting for model dependence versus not is not entirely surprising. The full data set in Experiment 1, with all of the model dependencies it includes, does include over-representation of certain features. However, because PCA is focused on maximizing total variance, this over-representation does get mitigated to an extent.

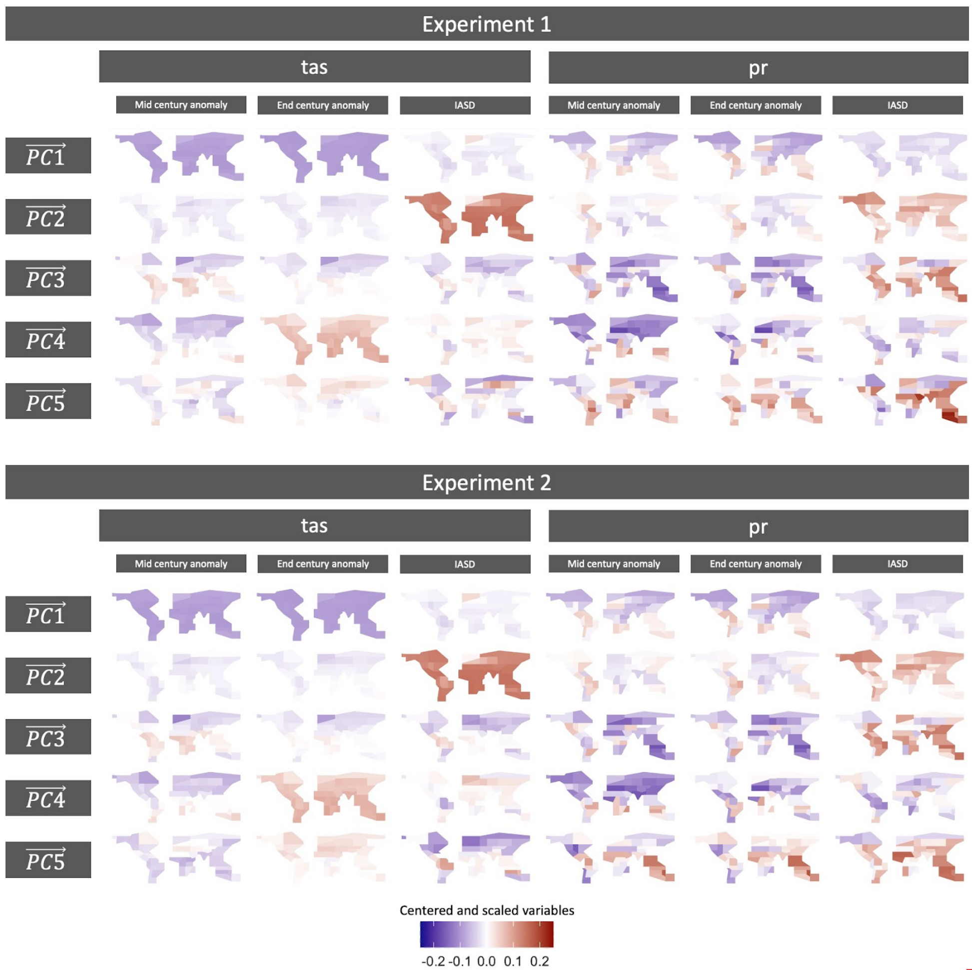

Figure 2: Maps of the first five eigenvectors of our full data. Each row is a single eigenvector, with maps presented for each of the indices. Note that the colorbar scales are all standardized. A larger, landscape-oriented version of this figure is included in Appendix A (Fig. A1) for easier inspection.

Deleted:

Deleted: six

By treating the span of these five eigenvectors as the representative space of full data, we can project all data into this space and visualize its behavior by two-dimensional plots of all five PCs combinations. Figure 3 shows these 2-d slices of the projection coefficients for each ESM/GCM and scenario into this space for each experiment. If an impact modeler wished, they could run every model-scenario combination here for all available ensemble members. In practice, however, this may not be computationally tractable to either run or analyze. This view also motivates our approach for selecting our subset of climate models that preserve the uncertainty characteristics defined by this space.

Deleted: Earth System Mode

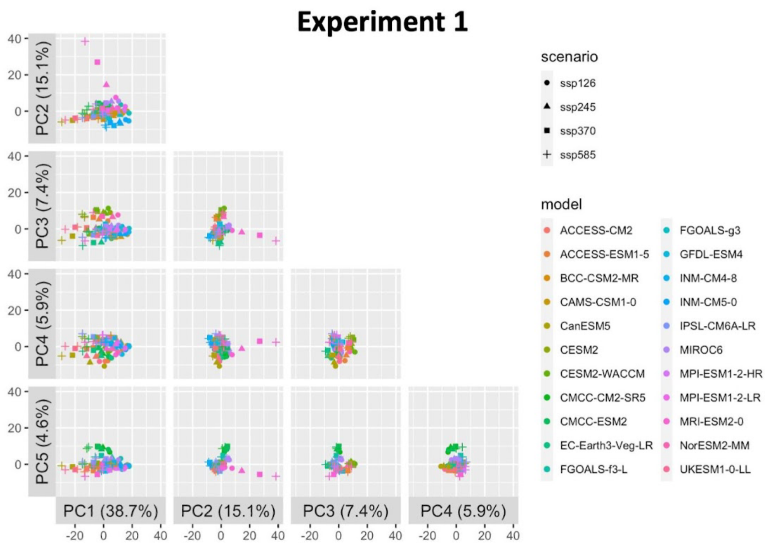
Experiment 1
scenario
ssp126
ssp245
ssp370
ssp585
model
ACCESS-CM2
ACCESS-ESM1-5
BCC-CSM2-MR
CAMS-CSM1-0
CanESM5
CESM2
CESM2-WACCM
CMCC-CM2-SR5
CMCC-ESM2
EC-Earth3-Veg-LR
FGOALS-f3-L
FGOALS-g3
GFDL-ESM4
INM-CM4-8
INM-CM5-0
IPSL-CM6A-LR
MIROC6
MPI-ESM1-2-HR
MPI-ESM1-2-LR
MRI-ESM2-0
NorESM2-MM
UKESM1-0-LL
PC1 (38.7%)
PC2 (15.1%)
PC3 (7.4%)
PC4 (5.9%)
PC5 (4.6%)

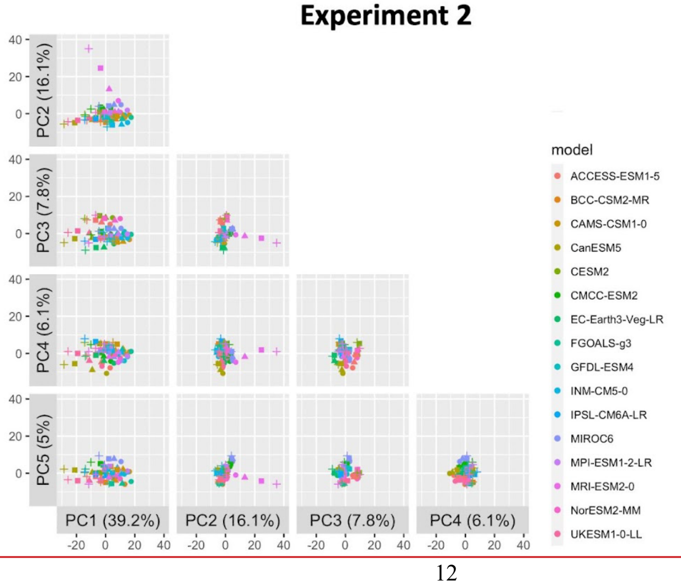
Experiment 2
model
ACCESS-ESM1-5
BCC-CSM2-MR
CAMS-CSM1-0
CanESM5
CESM2
CMCC-ESM2
EC-Earth3-Veg-LR
FGOALS-g3
GFDL-ESM4
INM-CM5-0
IPSL-CM6A-LR
MIROC6
MPI-ESM1-2-LR
MRI-ESM2-0
NorESM2-MM
UKESM1-0-LL
PC1 (39.2%)
PC2 (16.1%)
PC3 (7.8%)
PC4 (6.1%)
PC5 (5%)

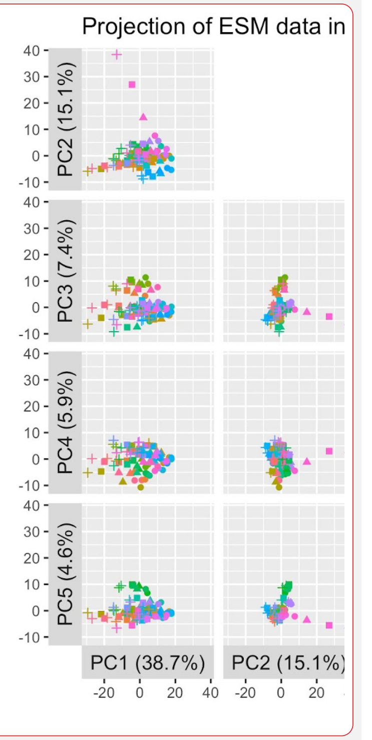
Projection of ESM data in
PC1 (38.7%)
PC2 (15.1%)
PC3 (7.4%)
PC4 (5.9%)
PC5 (4.6%)

Deleted:

Figure 3: 2-d slices of the projection coefficients for each ESM/GCM-scenario combination into the space spanned by the first five eigenvectors.

2.2 Selection criteria of subset of CMIP6 models

Once the full set of data has been projected into the new basis identified to maximize total variance by PCA (as in Figure 3), selecting a representative subset of climate models across that space is relatively straightforward, and so is adding additional selection criteria, like constraining the distribution of ECS values. The subset of climate models that minimizes distance to all other climate models across this five-dimensional space is the subset selected. In more detail, first, subsets of candidate models are formed (in this work, five models per subset, but the approach can be applied to any target subset size). While it would be possible to consider any combination of five models from the full set of 22, in this work we add a pre-filtering step. From all 22 choose 5 potential subsets, we only consider as candidate subsets the 72 subsets that roughly preserve the IPCC distribution of equilibrium climate sensitivity values and for which we could identify ECS values in the literature(Core Writing Team & (eds.), 2023; Lovato et al., 2022; Meehl et al., 2020). Then for each subset, we step through each non-candidate model and calculate the minimum Euclidean distance to any of the subset's climate model's coefficients. The summary metric for each subset of candidates is then the average over all non-candidate model minimum distances, and the subset of candidate models with the smallest summary metric is the selected subset. Unlike many metrics (e.g. (Nash & Sutcliffe, 1970; Tebaldi et al., 2020)), there is unfortunately not a clear threshold for 'good enough' performance based on this metric and so in the so in the next section, we provide a qualitative evaluation framework that assesses whether the selected subset is successful at preserving the major characteristics of the full ensemble's uncertainty characteristics.

2.3 Method for subset evaluation

The Hawkins and Sutton breakdown of total variance into relative sources of uncertainty inspired our choices of regional indices, both anomalies and interannual standard deviations. However, our subset selection is made in the space of the climate models' absolute positions, without formally considering the relative breakdowns into fraction of total variance explained by model uncertainty, scenario uncertainty, and internal variability. Therefore, the partitioning of *relative* uncertainty calculated in the style of Hawkins and Sutton (Hawkins & Sutton, 2009, 2011) is a useful independent framework to evaluate the extent to which our climate model subset preserves the characteristics of the full ensemble. We don't expect perfect agreement in the Hawkins and Sutton (HS) fractions between our climate model subset and the full data because we do change the distribution of ECS values in the subset we select. However, even qualitative discrepancies in the HS fractions between the full ensemble and the chosen subset can be useful to understand whether decisions such as constraining the distribution of ECS values are moving the relative contribution of each source of uncertainty in an explainable way.

Deleted: ESM
Deleted: ¶
Deleted: ESMs
Deleted: ¶
Formatted: Heading 2
Deleted: ESMs
Deleted: ESMs
Deleted: ESMs
Deleted: ESM
Deleted: number of ESMs that we
Deleted: as our
Deleted: 5 ESM
Deleted: of ESMs those
Deleted: ; Scafetta, 2022
Deleted: ESM
Deleted: candidate
Deleted: ESM's
Deleted: ESM
Deleted: ESMs
Deleted: results section, we provide further validation that the selected subset of ESMs for this setup is successful at preserving many of the major characteristics of the full data's uncertainty characterizations.¶
Formatted: Font: (Default) +Body (Times New Roman)

The calculations of HS fractions are as follows: Consider a set of trajectories for a given climate variable produced by various model ESMs and scenarios. For example, this could be the annual average temperature or precipitation in a given world region. At each time step, *t*, there will be variation in the estimates from each observation in the set. The goal for a given set is to attribute a proportion of the variation or uncertainty at each time step to one of the three sources: interannual variation, model uncertainty, and scenario uncertainty. In our application, we want to do this for a "full" model set and compare the distribution of assigned variance to the same analysis on a selected subset of models.

The crux of this method for separating uncertainty is to write the raw predictions for each observation as $X_{m,s,t} = x_{m,s,t} + i_{m,s} + \varepsilon_{m,s,t}$, where $X_{m,s,t}$ is the raw prediction for model *m* scenario *s* at time *t*, $x_{m,s,t}$ is a smoothed fit of the variable anomaly with reference period 1995-2014, $i_{m,s}$ is the average variable value over the reference period, and $\varepsilon_{m,s,t}$ is the residual, representing interannual variation. Note that while internal variability is itself a constant value for each climate model-scenario, the fraction of total variance that internal variability explains can change over time as the model and scenario components change. Similarly, while we do not want to select subsets of scenarios, understanding the relative contribution of scenario uncertainty is critical to appreciate the variability across the different models.

We can then essentially calculate the interannual variation component as the variance of all ε, the model uncertainty component at each time step as the variation in x over the different models, and the scenario uncertainty at each time step as the variation in x over the different scenarios. The variance calculations can have a weighting component, although in this work we treat all models included in each experiment-specific full ensemble as uniformly weighted. The interannual variability component is computed as $V = \sum_m var_{s,t}(\varepsilon_{m,s,t})$. The model uncertainty component is $M(t) = \frac{1}{N_s}\sum_s var_m(x_{m,s,t})$ for the number of scenarios used N_s (four in this study). The scenario uncertainty component is $S(t) = var_s(\sum_m x_{m,s,t})$.

Note that each of these components may, for example, be weighted based on each climate model's closeness to some observational set, but in this work we weight them uniformly, as we are not concerned with model validation. Furthermore, following the assertion by Hawkins and Sutton (2009) assert that final fractions of total variability are not strongly affected by using different weights.

Deleted: Table 2. Summary of method

Deleted: Step ... [1]

3 Results and discussion

The selected subset of ESM/GCMs and their respective ECS values are provided in Table 3 for each experiment. Figure 4 presents an identical plot to Fig. 3 but with the selected ESM/GCMs highlighted

Deleted: and Fig

Deleted: .

Deleted: , which is

Deleted:

by black box outlines to emphasize the extent to which the subset covers the full ensemble. We also perform a validation exercise based on the work of Hawkins and Sutton (Hawkins & Sutton, 2009, 2011) using the whole time series data rather than the 6 metrics that guided our subset selection to provide an additional perspective on the ability of the method to preserve the characteristics of variability of the whole ensemble.

Table 3. Selected Model subset and ECS values for each experiment. Models selected in both experiments in bold.

Experiment 1 Model (ECS value)	**Experiment 2 Model (ECS value)**
ACCESS-CM2 (4.70)	IPSL-CM6A-LR (4.6)
ACCESS-ESM1-5 (3.9)	**ACCESS-ESM1-5 (3.9)**
MRI-ESM2-0 (3.2)	**MRI-ESM2-0 (3.2)**
BCC-CSM2-MR (3.0)	MPI-ESM1-2-0 (3.0)
MIROC6 (2.6)	**MIROC6 (2.6)**

Deleted: We provide more quantitative validation in Section 3.1 based on the work of Hawkins and Sutton (Hawkins & Sutton, 2009, 2011).

Deleted: **Table 3. Selected ESM subset and ECS values** **ESM** ... [2]

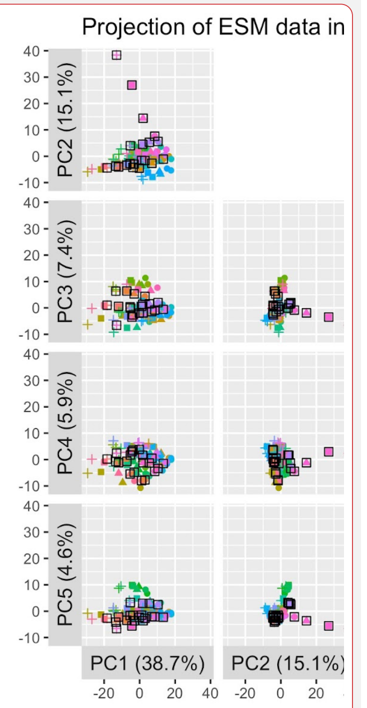

Deleted:

Formatted: Normal

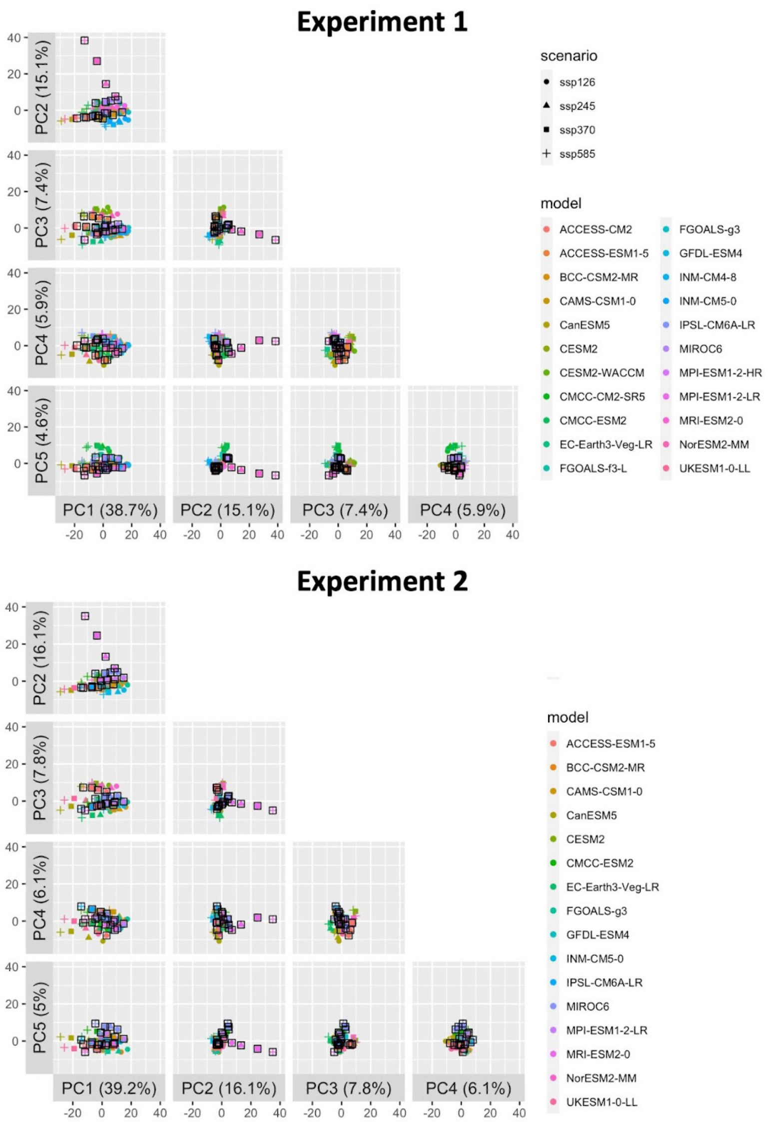
Experiment 1
scenario
ssp126
ssp245
ssp370
ssp585
model
ACCESS-CM2
ACCESS-ESM1-5
BCC-CSM2-MR
CAMS-CSM1-0
CanESM5
CESM2
CESM2-WACCM
CMCC-CM2-SR5
CMCC-ESM2
EC-Earth3-Veg-LR
FGOALS-f3-L
FGOALS-g3
GFDL-ESM4
INM-CM4-8
INM-CM5-0
IPSL-CM6A-LR
MIROC6
MPI-ESM1-2-HR
MPI-ESM1-2-LR
MRI-ESM2-0
NorESM2-MM
UKESM1-0-LL
PC2 (15.1%)
PC3 (7.4%)
PC4 (5.9%)
PC5 (4.6%)
PC1 (38.7%)
PC2 (15.1%)
PC3 (7.4%)
PC4 (5.9%)
Experiment 2
model
ACCESS-ESM1-5
BCC-CSM2-MR
CAMS-CSM1-0
CanESM5
CESM2
CMCC-ESM2
EC-Earth3-Veg-LR
FGOALS-g3
GFDL-ESM4
INM-CM5-0
IPSL-CM6A-LR
MIROC6
MPI-ESM1-2-LR
MRI-ESM2-0
NorESM2-MM
UKESM1-0-LL
PC2 (16.1%)
PC3 (7.8%)
PC4 (6.1%)
PC5 (5%)
PC1 (39.2%)
PC2 (16.1%)
PC3 (7.8%)
PC4 (6.1%)

Figure 4: Same as Figure 3 but with the selected ESM/GCMs highlighted by black box outlines or Experiment 1 (top) and Experiment 2 (bottom).

3.1 Subset Evaluation

As noted in Section 2.3, the partitioning of total variance into the relative contribution of different sources calculated by Hawkins and Sutton (Hawkins & Sutton, 2009, 2011) is a useful independent framework to evaluate the extent to which our climate model subset preserves the characteristics of the full ensemble. As we did not calculate the specific time series of Hawkins and Sutton (HS) fractions for internal variability (there, as here, quantified as interannual variability after detrending the annual mean time series), scenario uncertainty, and model uncertainty to form any part of our selection procedure, we can use these HS fractions as independent evaluation criteria. We calculate the time series of HS fractions for temperature and precipitation separately in each region, for the full set of data and over just our selected subset of data, i.e., for each experiment, over the selection of CMIP6 models making up the full data set in that experiment, and only using the subset of 5 ESM/GCMs that our method identified. Details of these calculations are provided in Section 2.3. To manage the inspection of three time series for each of 86 region-variable combinations, we use root mean square error (RMSE) to compare the full data time series and the subset data time series from 2040 onward (as that is the focus of our indices) for each uncertainty partition, for each variable in each region.

To identify specific region-variable combinations that are due for closer inspection, we set a threshold on the RMSE values for each uncertainty partition for each region-variable combination. As we note in Section 2.3, a discrepancy between the HS fractions for the subset and the full data is not a sign of poor selection. Rather, it merely means it is a region to inspect more closely and consider whether the discrepancies follow from our constraint of ECS values as part of our selection procedure. If any of the three uncertainty partitions have RMSE>0.1, we flag that region-variable combination for closer inspection. While thresholds like this are often arbitrary to set, each uncertainty partition for the subset data explaining the fraction of total variance within 10% of the full data's partition seems a good place to start. We show in Appendix A the results of a less stringent choice, namely, if we relax this to 20%, far fewer regions-variables get flagged for inspection in each experiment. Lowering this inspection threshold will of course flag more region-variables combinations, but as we point out below, a portion of the combinations flagged with a threshold of 0.1 still actually perform reasonably when plotted over time. Figure 5 provides a color-coded map of regions where temperature, precipitation, both, or neither have RMSE <= 0.1 for all three uncertainty partitions to give a sense of the spatial extent of performance.

Deleted: ¶

Deleted: .

Deleted: Validation

Deleted: the introduction

Deleted: uncertainty

Deleted: was critical in motivating this work and selecting regional indices of ESM behavior that address the different partitions for both temperature and precipitation. As we did not

Deleted: validation

Deleted: full CMIP6 ensemble

Deleted: we started from

Deleted: Appendix B.

Deleted: 54 of the 86 total region-variable combinations perform well based on this criterion alone. Note that many of these through Europe and East Asia are significant agricultural producers, regions where impacts often have critical implications for other regions and sectors in an integrated, multisectoral system.

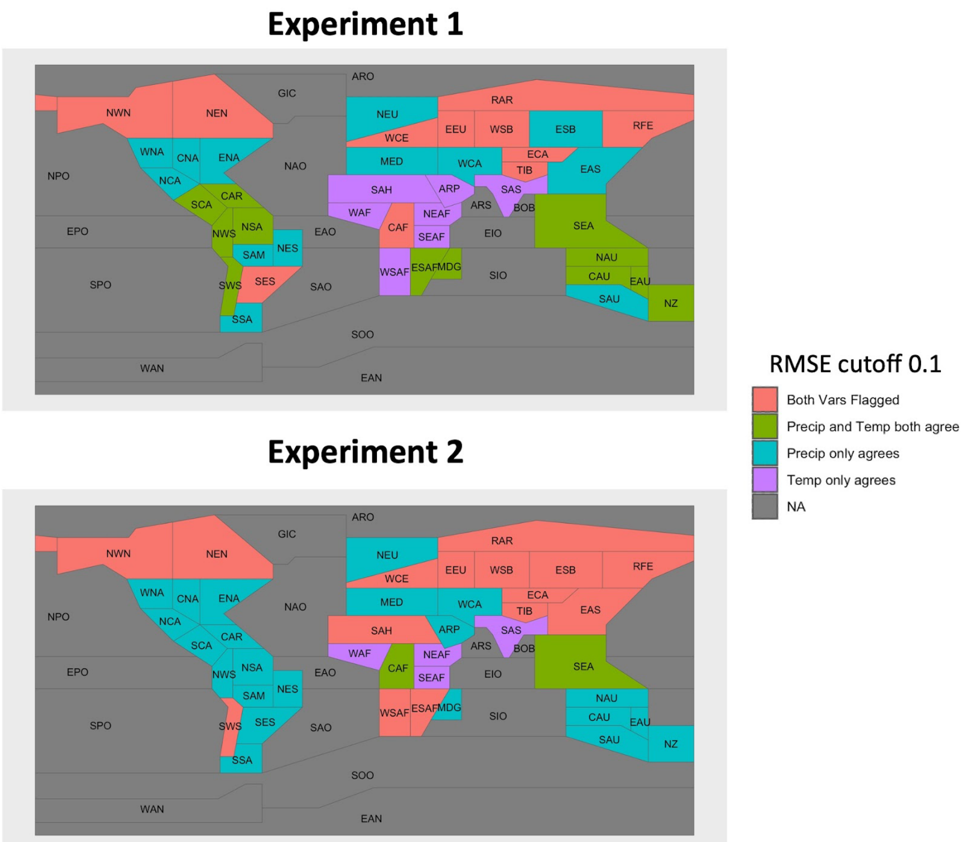

Figure 5. a color-coded map of regions where temperature, precipitation, both, or neither have RMSE <= 0.1 for all three uncertainty partitions.

The time series of HS fractions for the remaining region-variable combinations for which RMSE > 0.1 are plotted in Figure 6 (temperature) and Figure 7 (precipitation). For temperature in both experiments, we see that interannual variability is often performing well, with increasingly better performance over time. The partitioning of model and scenario uncertainty is where the subset's behavior begins to depart from the full data, although this too tends to have smaller discrepancies as time goes on. This is not

Deleted:

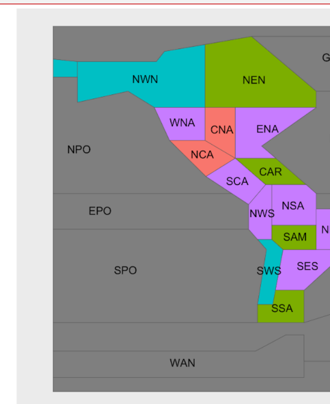

Deleted: 32

Deleted: in 14 regions

Deleted: in 18 regions bottom panel

Deleted: e

Deleted: over time?

Deleted: of ESMs

surprising: in the full set of data, a good portion of model uncertainty is driven by different ECS values. As provided in Table 2, the values across ESM/GCMs that participated in Tier 1 ScenarioMIP experiments do not match the IPCC very likely distribution. By contrast, we are only selecting subsets of ESM/GCMs that match this distribution, overall resulting in a cooler collection of climate models than the full data. This accounts for much of the discrepancy in the balance between scenario and model uncertainty contributions being different between our full and our subset data. Enforcing a different distribution of ECS values in the selected subset relative to the full data will also explain many of the discrepancies for precipitation, given the known strong correlation between temperature and precipitation changes. For precipitation, we overall see total uncertainty in the subset having a greater fraction explained by interannual variability and less by model uncertainty across time. For both temperature and precipitation, the direction of these discrepancies is not surprising given our choice to reshape the distribution of ECS to an overall cooler collection than the full data. What we want to see in all panels of Figures 6 and 7, is a qualitative agreement with the relevance of the three sources of uncertainty in the full ensemble. According to this criterion, most of the regions flagged by the application of the 0.1 threshold remain consistent with the full ensemble representation of the three uncertainty sources, for both variables and across both experiments.

Deleted: 1

Deleted: t

Deleted: accounting for the departure.

Deleted: , rather

Deleted: .

Deleted: Most frequently, regions feature a larger portion from interannual variability and a lesser portion from model uncertainty, again not surprisingly given our choice to reshape the distribution of ECS. For many of these regions (CNA, EAU, EEU, MDG, NAU, NCA, NSA, NWS, SCA, SES, WNA, WSB) the behavior of our subset approximates the full ensemble increasingly better as we move towards the later portion of the century. In Appendix A, we show the effect of relaxing the threshold to 0.2, resulting in nearly the full set of region/variable combinations passing our test (Fig. A2-A4).

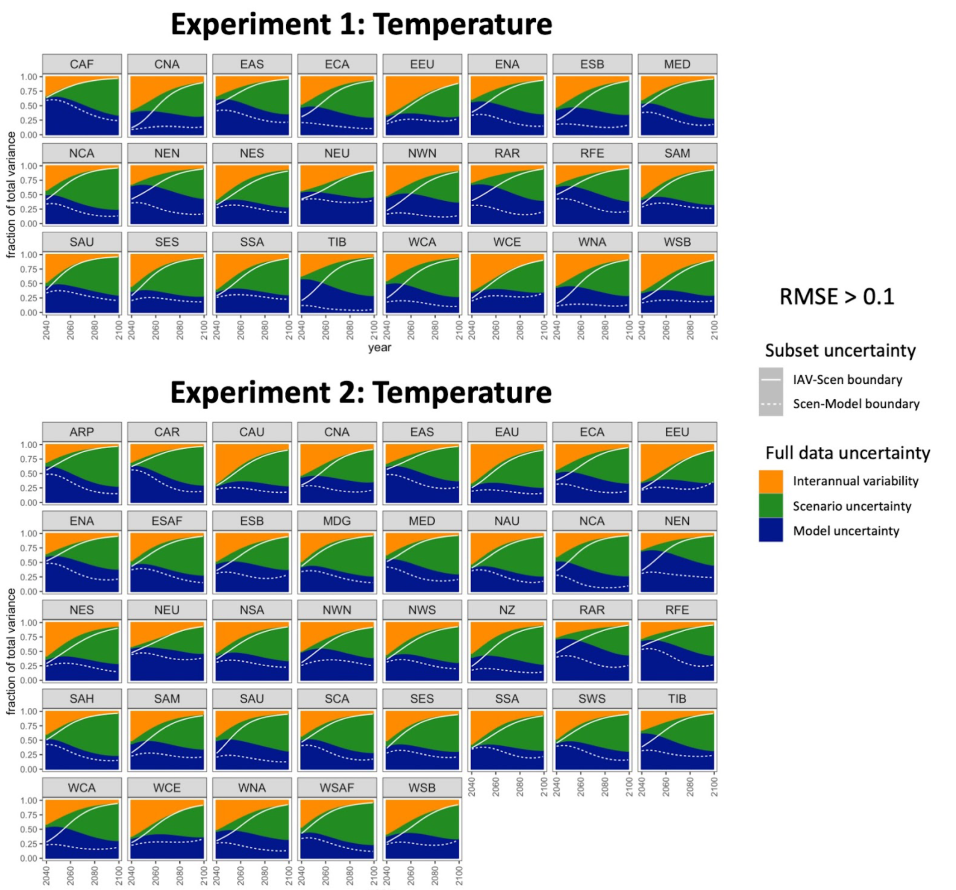

Figure 6: Regions flagged for closer inspection of their HS fraction time series for temperature. The color-blocked time series are the HS fractions from the full set of data, and the white curves overlaid are the respective boundaries for the subset data's uncertainty partitions.

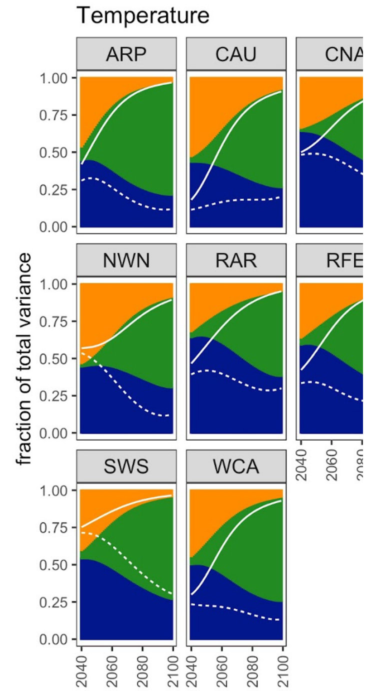

Deleted:

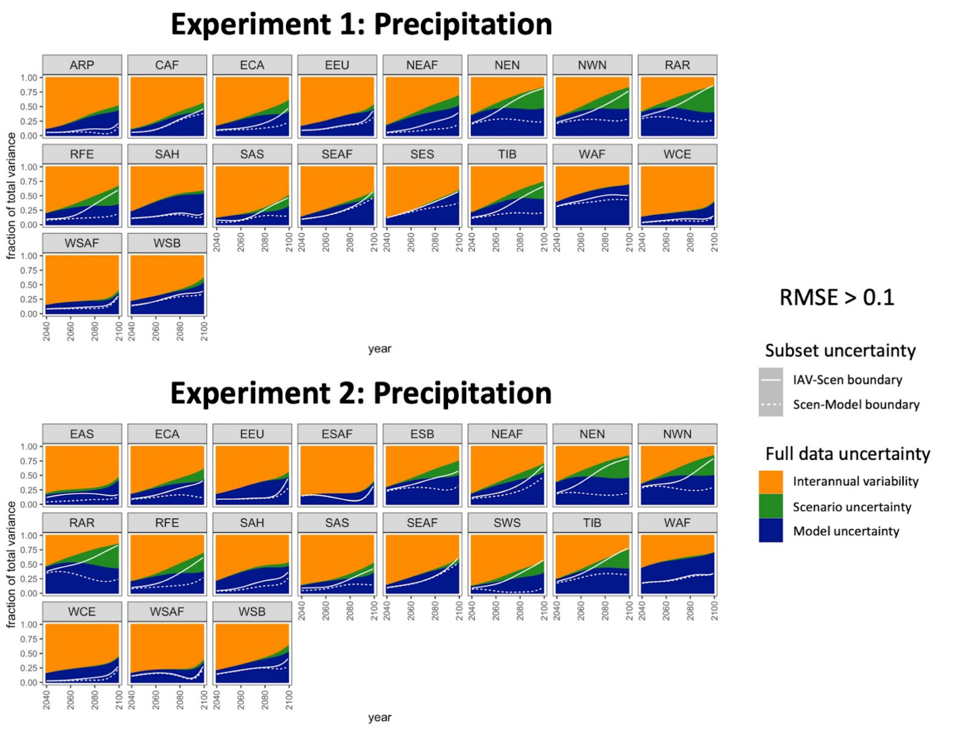

Figure 7: Same as Figure 6 but for precipitation.

Deleted:

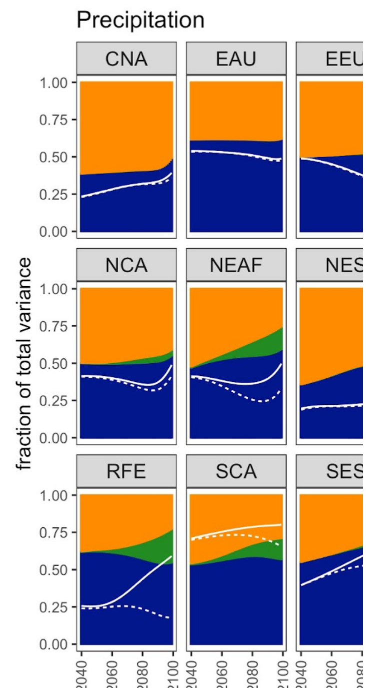

4 Conclusions

This work outlines and documents the success of a method for selecting a subset of climate models from CMIP6 that overall preserve the uncertainty characteristics of the full CMIP ensemble, particularly for use with multisectoral dynamics models that require global coverage and consistency across regions. Our methodology relies on pre-identifying regional indices of behavior for ESM/GCM output variables, as well as other filters (such as preserving the IPCC distribution of ECS values) judged to be critical for the robustness of impact and multisectoral modeling. With these assumptions, far fewer climate inputs

Deleted: ESMs

Deleted: set of CMIP data

Deleted: prioritizing

Deleted: that are key to impact and multisectoral models are needed to span the range of uncertainties seen in CMIP6, resulting in fewer impact model runs needing to be performed and analyzed. There are likely many situations in which a modeler could adapt the details of the method (outlined in Table 1) and code for their purposes, re-run to identify a subset of climate models, and validate that new subset in much less time and with much fewer computing resources needed than simply running impact models with all scenarios and ensemble members available for the 22 ESM/GCMs documented in Table 2. For multisectoral modelers integrating multiple different impacts, or running large ensemble experiments, the time saved only grows, even when accounting for method adjustment and re-validation of results. For researchers focused on emulators, there may be opportunities to identify fewer climate models that would benefit from generating more initial condition ensemble members, focusing efforts. Finally, Earth system modelers can gain new insights into their individual climate models by adding the approach to uncertainty characterization outlined in this work to their existing analyses.

The methodology outlined in this paper is an adaptable approach to both retain the major uncertainty characteristics of a large collection of global-coverage climate model data and to make changes (as we did to the full ensemble ECS distribution). While there are resulting regions for both temperature and precipitation where the uncertainty partitions of the subset of ESM/GCMs differ from the full set of CMIP6 models, these differences are primarily expected based on the different ECS distribution represented by our subset ESM/GCMs compared to the full data. For those interested in using our chosen subset, we hope that by providing detailed information about where the subset differs in Figures 5-7, impact modelers may be able to infer how results would change if the full set of data were used, with far lower computational burden than running all available data. Further, because the method is adaptable, an impact modeler particularly interested in a specific region could weight the outcomes in that region more heavily for selection of the subset.

As noted, this work is primarily coming from the perspective of a multisectoral dynamics modeler requiring global coverage of a range of climate model output variables at different time scales, and naturally other perspectives will come with their own caveats. Impacts can be estimated and worked with at a range of spatial scales; impact modelers concerned with finer scale or local impacts, or modelers focused on a single region rather than global coverage, may very well be served by prioritizing other factors like skill in their climate model subselection. Bias correction and downscaling are also tools heavily used to get to these finer spatial scales, and these processes introduce their own sources of uncertainty, particularly for very local phenomenon and over complex terrain (Kendon et al. 2010; Mearns et al. 2013; Barsugli et al. 2013; Lafferty and Sriver 2023). Generally, the method outlined in this work is more appropriate to work with raw CMIP6 data in its native resolutions or an ensemble of bias-adjusted and downscaled climate data that has been processed using a consistent bias-adjustment and downscaling method. On a final note for adaptations of this method, we focused on temperature and precipitation because many variables used in impacts modeling are correlated to or derived from these variables. This is especially true in agriculture, e.g. Sinha et al. 2023; Sinha et al. 2023; Peterson and Abatzoglou 2014; Allstadt et al. 2015; Gerst et al. 2020, although it holds in other sectors as well. One area for potential expansion of this method that would have more direct relevance to those derived variables would be to incorporate a time dimension more explicitly.

Deleted: 2

Deleted: ESMs

Deleted: 1

Deleted: ¶

Deleted: For Earth system modelers

Deleted: ESMs

Deleted: running

Deleted: . If all modeling centers performed a small number of ensemble members for a set of scenarios, this analysis could be repeated to identify specific models to run more ensemble members for. This can result in more efficient allocation of total computing resources in a model intercomparison exercise., focusing efforts.

Deleted: ESM

Deleted: ESM

Deleted: We

Formatted: Normal (Web)

Formatted: Default Paragraph Font, Font color: Auto

Deleted: ¶

Appendix A Additional figures

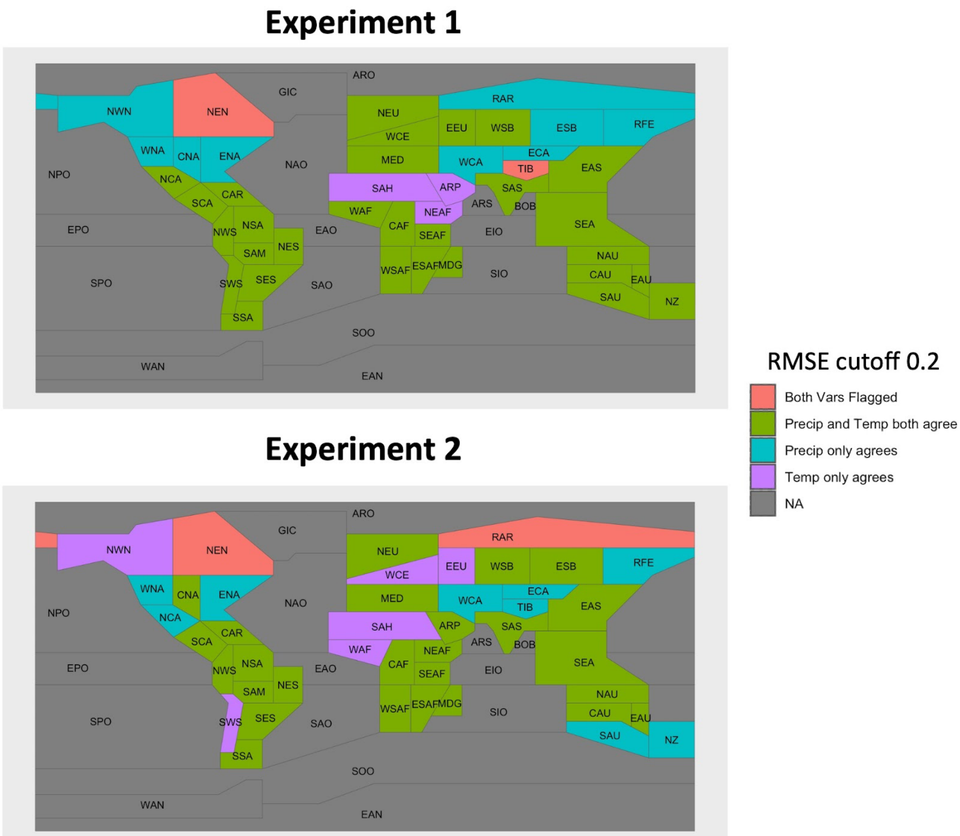

Figure A1: A color-coded map of regions where temperature, precipitation, both, or neither have RMSE <= 0.2 for all three uncertainty partitions.

Moved down [1]: Appendix A Additional figures

Moved (insertion) [1]

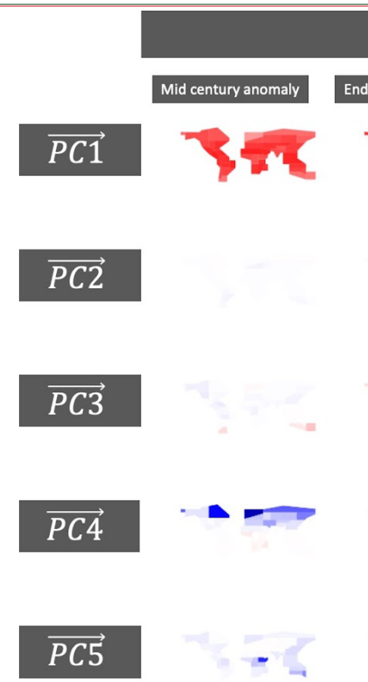

Deleted: ... [3]

Deleted:

Deleted:

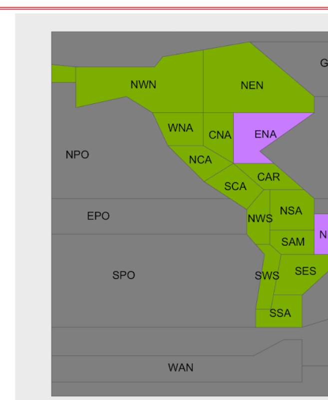

Deleted:

Deleted: 2

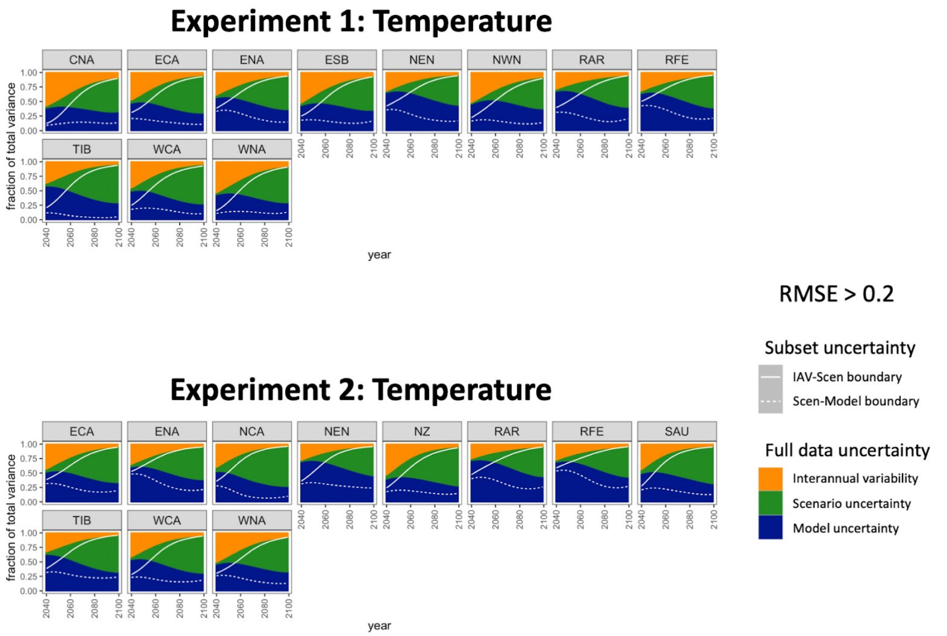

Figure A2: Same as Figure 6 but for RMS > 0.2 rather than 0.1

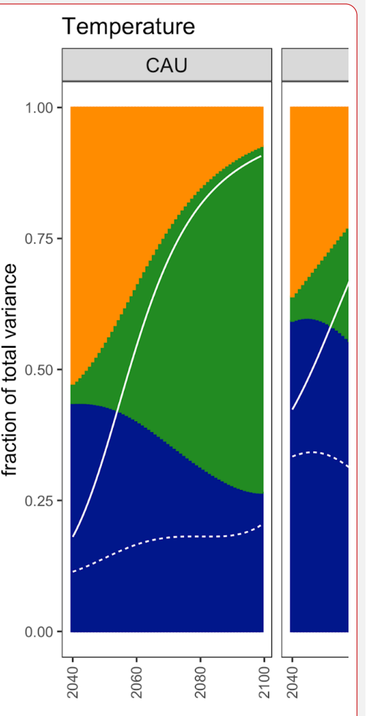

Deleted:

Deleted: 3

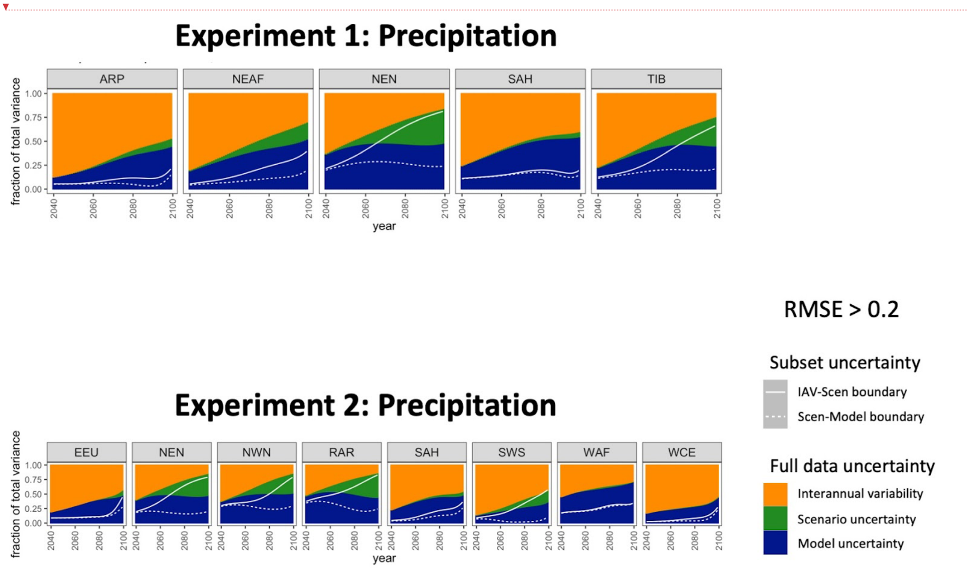

Figure A3: Same as Figure 7 but for RMS > 0.2 rather than 0.1.

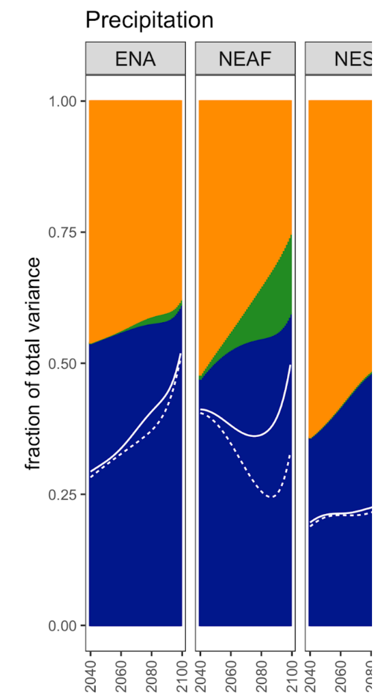

Deleted:

Deleted: 4

Code and data availability: All code and data are available via a Github metarepository (https://github.com/JGCRI/SnyderEtAl2023_uncertainty_informed_curation_metarepo) and minted with a permanent DOI (https://doi.org/10.57931/2223040)

Author contributions: CT conceived of the project, AS led design of the methodology and performed analysis, NP performed analysis, KD provided data; all authors contributed to methodology, analysis, and the writing of the paper.

Competing interests: The authors declare that they have no conflict of interest.

Acknowledgements: This research was supported by the U.S. Department of Energy, Office of Science, as part of research in MultiSector Dynamics, Earth and Environmental System Modeling Program. The Pacific Northwest National Laboratory is operated for DOE by Battelle Memorial Institute under contract DE-AC05-76RL01830. The views and opinions expressed in this paper are those of the authors alone.

References

Abramowitz, Gab, Nadja Herger, Ethan Gutmann, Dorit Hammerling, Reto Knutti, Martin Leduc, Ruth Lorenz, Robert Pincus, and Gavin A. Schmidt. 2019. "ESD Reviews: Model Dependence in Multi-Model Climate Ensembles: Weighting, Sub-Selection and out-of-Sample Testing." *Earth System Dynamics* 10 (1): 91–105.

Allstadt, Andrew J., Stephen J. Vavrus, Patricia J. Heglund, Anna M. Pidgeon, Wayne E. Thogmartin, and Volker C. Radeloff. 2015. "Spring Plant Phenology and False Springs in the Conterminous US during the 21st Century." *Environmental Research Letters: ERL [Web Site]* 10 (10): 104008.

Barsugli, Joseph J., Galina Guentchev, Radley M. Horton, Andrew Wood, Linda O. Mearns, Xin-Zhong Liang, Julie A. Winkler, et al. 2013. "The Practitioner's Dilemma: How to Assess the Credibility of Downscaled Climate Projections." *Eos* 94 (46): 424–25.

Beusch, L., Gudmundsson, L., & Seneviratne, S. I. (2020). Emulating Earth system model temperatures with MESMER: from global mean temperature trajectories to grid-point-level realizations on land. *Earth System Dynamics*, *11*(1), 139–159.

Brands, Swen. 2022. "A Circulation-Based Performance Atlas of the CMIP5 and 6 Models for Regional Climate Studies in the Northern Hemisphere Mid-to-High Latitudes." *Geoscientific Model Development* 15 (4): 1375–1411.

Core Writing Team, H. Lee and J. Romero (eds.). 2023. "IPCC, 2023: Summary for Policymakers. In: Climate Change 2023: Synthesis Report. Contribution of Working Groups I, II and III to the Sixth Assessment Report of the Intergovernmental Panel on Climate Change." https://doi.org/10.59327/IPCC/AR6-9789291691647.001.

Deleted: Appendix B Hawkins and Sutton uncertainty calculations

Consider a set of trajectories for a given climate variable produced by various ESMs and scenarios. For example, this could be the annual average temperature or precipitation in a given world region. At each time step, *t*, there will be variation in the estimates from each observation in the set. The goal for a given set is to attribute a proportion of the variation or uncertainty at each time step to one of the three sources: interannual variation, model uncertainty, and scenario uncertainty. In our application, we want to do this for a "full" model set and compare the distribution of assigned variance to the same analysis on a selected subset of models.

The crux of this method for separating uncertainty is to write the raw predictions for each observation as $X_{m,s,t} = x_{m,s,t} + i_{m,s} + \varepsilon_{m,s,t}$, where $X_{m,s,t}$ is the raw prediction for model *m* scenario *s* at time *t*, $x_{m,s,t}$ s a smoothed fit of the variable anomaly with reference period 1995-2014, $i_{m,s}$ is the average variable value over the reference period, and $\varepsilon_{m,s,t}$ is the residual, representing interannual variation.

We can then essentially calculate the interannual variation component as the variance of all ε, the model uncertainty component at each time step as the variation in *x* over the different models, and the scenario uncertainty at each time step as the variation in *x* over the different scenarios. The variance calculations each have a weighting component. Models who more closely match the trend of observational data (W5E5v2.0 (Lange et al., 2021)) over the historic period will have their observations hold more weight. The weighting is as follows: $w_m = \frac{1}{x_{obs}+|x_m - x_{obs}|}$, where x_{obs} is the warming observed from 1995-2014 in the observation dataset (calculated as the difference in the smooth fit polynomial at the ends of that period), and x_m is the same thing but for the given model *m*. Weights are normalized ($W_m = \frac{w_m}{\sum_m w_m}$) to give the interannual variability component $V = \sum_m W_m \, var_{s,t}(\varepsilon_{m,s,t})$. The model uncertainty component is $M(t) = \frac{1}{N_s}\sum_s var_m^W(x_{m,s,t})$ for the number of scenarios used N_s (four in this study) and using the weighted variance function (var^W). The scenario uncertainty component is $S(t) = var_s(\sum_m W_m \, x_{m,s,t})$.

Formatted: Default Paragraph Font

Formatted: Default Paragraph Font

Formatted: Default Paragraph Font

Formatted: Default Paragraph Font

Formatted: Default Paragraph Font

Dolan, F., Lamontagne, J., Calvin, K., Snyder, A., Narayan, K. B., Di Vittorio, A. V., & Vernon, C. R. (2022). Modeling the economic and environmental impacts of land scarcity under deep uncertainty. *Earth's Future*, *10*(2), e2021EF002466.

Dolan, F., Lamontagne, J., Link, R., Hejazi, M., Reed, P., & Edmonds, J. (2021). Evaluating the economic impact of water scarcity in a changing world. *Nature Communications*, *12*(1), 1915.

Eyring, V., Bony, S., Meehl, G. A., Senior, C. A., Stevens, B., Stouffer, R. J., & Taylor, K. E. (2016). Overview of the Coupled Model Intercomparison Project Phase 6 (CMIP6) experimental design and organization. *Geoscientific Model Development*, *9*(5), 1937–1958. https://doi.org/10.5194/gmd-9-1937-2016

Frieler, K., Lange, S., Piontek, F., Reyer, C. P. O., Schewe, J., Warszawski, L., Zhao, F., Chini, L., Denvil, S., Emanuel, K., & Others. (2017). Assessing the impacts of 1.5 C global warming--simulation protocol of the Inter-Sectoral Impact Model Intercomparison Project (ISIMIP2b). *Geoscientific Model Development*, *10*(12), 4321–4345.

Graham, N. T., Hejazi, M. I., Chen, M., Davies, E. G. R., Edmonds, J. A., Kim, S. H., Turner, S. W. D., Li, X., Vernon, C. R., Calvin, K., & Others. (2020). Humans drive future water scarcity changes across all Shared Socioeconomic Pathways. *Environmental Research Letters: ERL [Web Site]*, *15*(1), 014007.

Gerst, Katharine L., Theresa M. Crimmins, Erin E. Posthumus, Alyssa H. Rosemartin, and Mark D. Schwartz. 2020. "How Well Do the Spring Indices Predict Phenological Activity across Plant Species?" *International Journal of Biometeorology* 64 (5): 889–901.

Guivarch, C., Le Gallic, T., Bauer, N., Fragkos, P., Huppmann, D., Jaxa-Rozen, M., Keppo, I., Kriegler, E., Krisztin, T., Marangoni, G., & Others. (2022). Using large ensembles of climate change mitigation scenarios for robust insights. *Nature Climate Change*, *12*(5), 428–435.

Hausfather, Zeke, Kate Marvel, Gavin A. Schmidt, John W. Nielsen-Gammon, and Mark Zelinka. 2022. "Climate Simulations: Recognize the 'hot Model' Problem." Nature Publishing Group UK. May 4, 2022. https://doi.org/10.1038/d41586-022-01192-2.

Hawkins, E., & Sutton, R. (2009). The potential to narrow uncertainty in regional climate predictions. *Bulletin of the American Meteorological Society*, *90*(8), 1095–1108.

Hawkins, E., & Sutton, R. (2011). The potential to narrow uncertainty in projections of regional precipitation change. *Climate Dynamics*, *37*, 407–418.

Iturbide, M., Fernández, J., Gutiérrez, J. M., Pirani, A., Huard, D., Al Khourdajie, A., Baño-Medina, J., Bedia, J., Casanueva, A., Cimadevilla, E., & Others. (2022). Implementation of FAIR principles in the IPCC: the WGI AR6 Atlas repository. *Scientific Data*, *9*(1), 629.

Lange, S. (2019). Trend-preserving bias adjustment and statistical downscaling with ISIMIP3BASD (v1. 0). *Geoscientific Model Development*, *12*(7), 3055–3070.

Kendon, Elizabeth J., Richard G. Jones, Erik Kjellström, and James M. Murphy. 2010. "Using and Designing GCM–RCM Ensemble Regional Climate Projections." *Journal of Climate* 23 (24): 6485–6503.

Lafferty, David C., and Ryan L. Sriver. 2023. "Downscaling and Bias-Correction Contribute Considerable Uncertainty to Local Climate Projections in CMIP6." *Npj Climate and Atmospheric Science* 6 (1): 1–13.

Deleted: Core Writing Team, H. L., & (eds.), J. R. (2023). *IPCC, 2023: Summary for Policymakers. In: Climate Change 2023: Synthesis Report. Contribution of Working Groups I, II and III to the Sixth Assessment Report of the Intergovernmental Panel on Climate Change*. https://doi.org/10.59327/IPCC/AR6-9789291691647.001

Formatted: Default Paragraph Font

Formatted: Default Paragraph Font

Formatted: Default Paragraph Font

Formatted: Default Paragraph Font

Lange, S., Menz, C., Gleixner, S., Cucchi, M., Weedon, G. P., Amici, A., Bellouin, N., Schmied, H. M., Hersbach, H., Buontempo, C., & Cagnazzo, C. (2021). *WFDE5 over land merged with ERA5 over the ocean (W5E5 v2.0)* [dataset]. ISIMIP Repository. https://doi.org/10.48364/ISIMIP.342217

Lehner, F., Deser, C., Maher, N., Marotzke, J., Fischer, E. M., Brunner, L., Knutti, R., & Hawkins, E. (2020). Partitioning climate projection uncertainty with multiple large ensembles and CMIP5/6. *Earth System Dynamics*, *11*(2), 491–508.

Lovato, T., Peano, D., Butenschön, M., Materia, S., Iovino, D., Scoccimarro, E., Fogli, P. G., Cherchi, A., Bellucci, A., Gualdi, S., & Others. (2022). CMIP6 simulations with the CMCC Earth system model (CMCC-ESM2). *Journal of Advances in Modeling Earth Systems*, *14*(3), e2021MS002814.

Mearns, L. O., S. Sain, L. R. Leung, M. S. Bukovsky, S. McGinnis, S. Biner, D. Caya, et al. 2013. "Climate Change Projections of the North American Regional Climate Change Assessment Program (NARCCAP)." *Climatic Change* 120 (4): 965–75.

Meehl, G. A., Senior, C. A., Eyring, V., Flato, G., Lamarque, J.-F., Stouffer, R. J., Taylor, K. E., & Schlund, M. (2020). Context for interpreting equilibrium climate sensitivity and transient climate response from the CMIP6 Earth system models. *Science Advances*, *6*(26), eaba1981.

Merrifield, A., L. Brunner, R. Lorenz, V. Humphrey, and R. Knutti. 2023. "Climate Model Selection by Independence, Performance, and Spread (ClimSIPS v1.0.1) for Regional Applications." *Geoscientific Model Development*, August. https://doi.org/10.5194/gmd-16-4715-2023.

Müller, C., Franke, J., Jägermeyr, J., Ruane, A. C., Elliott, J., Moyer, E., Heinke, J., Falloon, P. D., Folberth, C., Francois, L., & Others. (2021). Exploring uncertainties in global crop yield projections in a large ensemble of crop models and CMIP5 and CMIP6 climate scenarios. *Environmental Research Letters: ERL [Web Site]*, *16*(3), 034040.

Nash, J. E., & Sutcliffe, J. V. (1970). River flow forecasting through conceptual models part I—A discussion of principles. *Journal of Hydrology*, *10*(3), 282–290.

Nath, S., Lejeune, Q., Beusch, L., Seneviratne, S. I., & Schleussner, C.-F. (2022). MESMER-M: an Earth system model emulator for spatially resolved monthly temperature. *Earth System Dynamics*, *13*(2), 851–877.

O'Neill, B. C., Tebaldi, C., van Vuuren, D. P., Eyring, V., Friedlingstein, P., Hurtt, G., Knutti, R., Kriegler, E., Lamarque, J.-F., Lowe, J., Meehl, G. A., Moss, R., Riahi, K., & Sanderson, B. M. (2016). The Scenario Model Intercomparison Project (ScenarioMIP) for CMIP6. *Geoscientific Model Development*, *9*(9), 3461–3482. https://doi.org/10.5194/gmd-9-3461-2016

Parding, Kajsa M., Andreas Dobler, Carol F. McSweeney, Oskar A. Landgren, Rasmus Benestad, Helene B. Erlandsen, Abdelkader Mezghani, et al. 2020. "GCMeval – An Interactive Tool for Evaluation and Selection of Climate Model Ensembles." *Climate Services* 18 (100167): 100167.

Peterson, Alexander G., and John T. Abatzoglou. 2014. "Observed Changes in False Springs over the Contiguous United States." *Geophysical Research Letters* 41 (6): 2156–62.

Prudhomme, C., Giuntoli, I., Robinson, E. L., Clark, D. B., Arnell, N. W., Dankers, R., Fekete, B. M., Franssen, W., Gerten, D., Gosling, S. N., & Others. (2014). Hydrological droughts in the 21st century, hotspots and uncertainties from a global multimodel ensemble experiment. *Proceedings of the National Academy of Sciences*, *111*(9), 3262–3267.

Deleted: ¶

Formatted: Default Paragraph Font

Deleted: ¶

Formatted: Default Paragraph Font

Formatted: Default Paragraph Font

Formatted: Default Paragraph Font

Quilcaille, Y., Gudmundsson, L., Beusch, L., Hauser, M., & Seneviratne, S. I. (2022). Showcasing MESMER-X: Spatially Resolved Emulation of Annual Maximum Temperatures of Earth System Models. *Geophysical Research Letters*, *49*(17), e2022GL099012.

Rosenzweig, C., Elliott, J., Deryng, D., Ruane, A. C., Müller, C., Arneth, A., Boote, K. J., Folberth, C., Glotter, M., Khabarov, N., & Others. (2014). Assessing agricultural risks of climate change in the 21st century in a global gridded crop model intercomparison. *Proceedings of the National Academy of Sciences*, *111*(9), 3268–3273.

Rosenzweig, C., Jones, J. W., Hatfield, J. L., Ruane, A. C., Boote, K. J., Thorburn, P., Antle, J. M., Nelson, G. C., Porter, C., Janssen, S., & Others. (2013). The agricultural model intercomparison and improvement project (AgMIP): protocols and pilot studies. *Agricultural and Forest Meteorology*, *170*, 166–182.

Sinha, E., K. V. Calvin, and B. Bond-Lamberty. 2023. “Modeling Perennial Bioenergy Crops in the E3SM Land Model (ELMv2).” *Journal of Advances*. https://agupubs.onlinelibrary.wiley.com/doi/abs/10.1029/2022MS003171.

Sinha, Eva, Ben Bond-Lamberty, Katherine V. Calvin, Beth A. Drewniak, Gautam Bisht, Carl Bernacchi, Bethany J. Blakely, and Caitlin E. Moore. 2023. “The Impact of Crop Rotation and Spatially Varying Crop Parameters in the E3SM Land Model (ELMv2).” *Journal of Geophysical Research. Biogeosciences*, March. https://doi.org/10.1029/2022jg007187.

Tebaldi, C., Armbruster, A., Engler, H. P., & Link, R. (2020). Emulating climate extreme indices. *Environmental Research Letters: ERL [Web Site]*, *15*(7), 074006.

Tebaldi, C., Dorheim, K., Wehner, M., & Leung, R. (2021). Extreme metrics from large ensembles: investigating the effects of ensemble size on their estimates. *Earth System Dynamics*, *12*(4), 1427–1501.

Tebaldi, C., Snyder, A., & Dorheim, K. (2022). STITCHES: creating new scenarios of climate model output by stitching together pieces of existing simulations. *Earth System Dynamics*, 1–58. https://doi.org/10.5194/esd-2022-14

Warszawski, L., Frieler, K., Huber, V., Piontek, F., Serdeczny, O., & Schewe, J. (2014). The inter-sectoral impact model intercomparison project (ISI--MIP): project framework. *Proceedings of the National Academy of Sciences*, *111*(9), 3228–3232.

Formatted: Default Paragraph Font

Formatted: Default Paragraph Font

Deleted: Scafetta, N. (2022). Advanced Testing of Low, Medium, and High ECS CMIP6 GCM Simulations Versus ERA5-T2m. *Geophysical Research Letters*, *49*(6), e2022GL097716.

Page 14: [1] Deleted	**Snyder, Abigail C**	**6/10/24 11:57:00 AM**
Page 15: [2] Deleted	**Snyder, Abigail C**	**6/10/24 12:03:00 PM**
Page 23: [3] Deleted	**Snyder, Abigail C**	**6/10/24 12:13:00 PM**